Journal of Power Sources 225 (2013) 338–346

Contents lists available at SciVerse ScienceDirect

Journal of Power Sources

journal homepage: www.elsevier.com/locate/jpowsour

Enhanced electrochemical performance of LiF-modified $LiNi_{1/3}Co_{1/3}Mn_{1/3}O_2$ cathode materials for Li-ion batteries

S.J. Shi, J.P. Tu*, Y.Y. Tang, Y.Q. Zhang, X.Y. Liu, X.L. Wang, C.D. Gu

State Key Laboratory of Silicon Materials, Key Laboratory of Advanced Materials and Applications for Batteries of Zhejiang Province and Department of Materials Science and Engineering, Zhejiang University, Hangzhou 310027, China

HIGHLIGHTS

- ► $LiNi_{1/3}Co_{1/3}Mn_{1/3}O_2$ is modified with LiF by a wet chemical method.
- ► Discharge capacity of 137 mAh g^{-1} is obtained at 10 C (2800 mA g^{-1}).
- ► Capacity retention of 93.5% is obtained at 1 C at 60 °C after 50 cycles.
- ► Reversible capacity of 124.4 mAh g^{-1} is obtained at 1 C at 0 °C.
- ► Even at −20 °C, discharge capacity of 85.6 mAh g^{-1} is obtained at 0.1 C.

ARTICLE INFO

Article history:
Received 1 August 2012
Received in revised form
17 October 2012
Accepted 19 October 2012
Available online 29 October 2012

Keywords:
Layered oxide
Lithium fluoride
Surface modification
Lithium ion battery

ABSTRACT

LiF is successful used to modify the surface of layered $LiNi_{1/3}Co_{1/3}Mn_{1/3}O_2$ via a wet chemical method followed by an annealing process. The lattice structure of $LiNi_{1/3}Co_{1/3}Mn_{1/3}O_2$ is not changed distinctly after modification and part of F^- dopes into the surface lattice of the oxide. The LiF-modified oxide exhibits capacity retentions of 97.5% at 0.1 C at room temperature and 93.5% at 1 C at 60 °C after 50 cycles, and delivers a high discharge capacity of 137 mAh g^{-1} at 10 C at room temperature. Furthermore, it has reversible capacities of 124.4 mAh g^{-1} at 1 C at 0 °C and 85.6 mAh g^{-1} at 0.1 C at −20 °C, respectively. Cyclic voltammetry (CV) and electrochemical impedance spectroscopy (EIS) tests show that the LiF-modified layer can reduce the dissolution of metal ions in the electrode and enhance the conductivity of the oxide surface through partly F-substitution. LiF modification will be promising for the application of layered oxide for lithium ion batteries.

1. Introduction

Because of the drawbacks of $LiCoO_2$ such as high cost, toxicity of cobalt and so on, research and development of new cathode materials for lithium ion batteries are ongoing to replace it. Natural substitutes are $LiMnO_2$ and $LiNiO_2$. However, both of them are difficult to synthesize due to their unstable structure during calcination treatment. In addition, phase transition will easily happen during charge–discharge process, leading to poor cyclic performance [1,2]. Layered oxide $LiMO_2$ (M = Mn, Ni, Co) which has been widely investigated is deemed to be one of the most promising candidates of cathode materials [3–14]. However, the relatively poor cyclic performance at a high operating voltage (higher than 4.3 V) or high current density is one of its drawbacks and the mechanism of capacity fading has not yet been clarified [15].

It is reported that ion substitution can improve the electrochemical performances [16–18]. F-substitution and LiF addition of layered oxide $LiMO_2$ (M = Mn, Ni, Co) have been widely investigated and are proved to effectively enhance the cyclic stability [19–25]. However, LiF is mostly reported just as an addition for doping and seldom as a surface-modified material to improve the electrochemical performance of layered oxide $LiMO_2$ (M = Mn, Ni, Co). Although XPS analysis showed that the added LiF would move to the surface and exist as a surface layer [26], others considered that fluorine substitution for oxygen was effective since the changes in lattice parameters were observed [19,23,27,28].

In addition, surface modification of oxides, phosphates, carbon and fluorides have been proved to be an effective way to restrain the electrolyte decomposition on the surface of cathode materials and enhance the cyclic stability of layered oxide [29–34]. Among

* Corresponding author. Tel.: +86 571 87952856; fax: +86 571 87952573.
E-mail addresses: tujp@zju.edu.cn, tujplab@zju.edu.cn (J.P. Tu).

0378-7753/$ – see front matter © 2012 Elsevier B.V. All rights reserved.
http://dx.doi.org/10.1016/j.jpowsour.2012.10.065

them, fluorides are considered to directly protect the electrode materials from the HF attack resulting from the electrolyte [35,36]. AlF_3 [37], ZrF_x [38], SrF_2 [39] and CaF_2 [40] have been successfully coated on the surface of layered oxides and the electrochemical performances of the cathode material are significantly improved. LiF was also used to modify $LiMn_2O_4$ by Bai et al. [41], and an improvement of electrochemical performance was obtained even charged to 4.7 V and 4.9 V.

Here, in this present work, $LiNi_{1/3}Co_{1/3}Mn_{1/3}O_2$ which has been considered to be one of the most promising candidates for lithium ion battery among layered oxide $LiMO_2$ (M = Mn, Ni, Co) is chosen as research object [42–45]. And LiF is modified on the surface of $LiNi_{1/3}Co_{1/3}Mn_{1/3}O_2$ via a wet chemical method followed by annealing treatment. The electrochemical performances of the LiF-modified $LiNi_{1/3}Co_{1/3}Mn_{1/3}O_2$ are effectively improved not only at room temperature, but also at high or low temperatures. CV and EIS tests are carried out to further understand the effect of LiF modification on layered oxide cathode material.

2. Experimental

Layered $LiNi_{1/3}Co_{1/3}Mn_{1/3}O_2$ was synthesized via a high-temperature solid state reaction. Stoichiometric amounts of commercial precursor ($Mn_{1/3}Ni_{1/3}Co_{1/3}(OH)_2$) and 3 wt.% excess $LiOH\cdot H_2O$ were mixed thoroughly. Then, the mixture was calcined at 800 °C in a tube furnace for 16 h in air to get the oxide powder. The LiF coating was performed as follows: stoichiometric amounts of $LiNO_3$ and NH_4F were dissolved in deionized water to obtain a dilute solution, respectively. A desired amount of the oxide powder was dispersed in the $LiNO_3$ dilute solution. Then, the resulting mixture was heated to 70 °C and stirred vigorously. The NH_4F dilute solution was then added into the mixture drop by drop for more than 3 h. Continuous stirring was performed till the solution was evaporated to dryness. The obtained black powder was calcined at 500 °C in a tube furnace for 2 h in air and then cooled to room temperature at a speed of 2 °C min^{-1} to get the LiF-modified $LiMn_{1/3}Ni_{1/3}Co_{1/3}O_2$. The amount of LiF is 3 wt.% in the as-prepared material. The morphologies and microstructures of the as-synthesized powders were characterized using field emission scanning electron microscopy (FESEM, FEI SIRION) coupled with an X-ray energy dispersive spectroscope (EDS, BRUKER AXS), X-ray diffraction (XRD, Philips PC-APD with Cu Kα radiation), transmission electron microscopy (TEM, Tecnai G2 F30 S-Twin) and X-ray photoelectron spectroscopy (XPS).

The working electrodes were prepared by a slurry coating procedure. The slurry consisted of 85 wt.% as-synthesized materials, 10 wt.% carbon conductive agents (supper P) and 5 wt.% polyvinylidene fluoride (PVDF) was coated on aluminum foil. After drying at 90 °C for 24 h in vacuum, the sample was pressed under a pressure of 20 MPa. A metallic lithium foil served as the anode, 1 M $LiPF_6$ in ethylene carbonate (EC)-dimethyl carbonate (DMC) (1: 1 in volume) was used as the electrolyte, and a polypropylene microporous film (Cellgard 2300) as the separator. The cells were assembled in an argon-filled glove box with H_2O concentration below 1 ppm. The galvanostatic discharge–charge tests were performed with coin-type cells (CR2025) on a LAND battery program-control test system (Wuhan, China) between 2.5 and 4.5 V at rates from 0.1 to 10 C (1 C = 280 mA g^{-1}) at temperatures of −20–60 °C. CV tests were carried out on an electrochemical workstation (CHI660C) in the potential window of 2.5–4.8 V (vs. Li/Li^+) at a scan rate of 0.1 mV s^{-1}. EIS measurements were performed on this apparatus using a three-electrode cell with the oxide as the working electrode, metallic lithium foil as both the counter and reference electrodes. The amplitude of the AC signal was 5 mV over a frequency range from 100 kHz to 10 mHz at a charge state of 4.5 V.

3. Results and discussion

3.1. Material characterization

XRD patterns of $LiNi_{1/3}Co_{1/3}Mn_{1/3}O_2$ and $LiNi_{1/3}Co_{1/3}Mn_{1/3}O_2$/LiF powders are shown in Fig. 1. All the XRD patterns can be indexed to the hexagonal α-$NaFeO_2$ structure with R $m\bar{3}$ space group, and distinct splitting of (006)/(012) and (018)/(110) peaks indicates that these oxides possess a well-developed layered structure. Furthermore, all the reflections of $LiNi_{1/3}Co_{1/3}Mn_{1/3}O_2$/LiF correspond to the layered oxide and no peaks of LiF are present due to low quantity. The XRD patterns prove that the layered structure of $LiNi_{1/3}Co_{1/3}Mn_{1/3}O_2$ is not destroyed after LiF modification.

The morphologies of the layered oxides before and after LiF modification are shown in Fig. 2. The bare $LiMn_{1/3}Ni_{1/3}Co_{1/3}O_2$ is composed of ball-like secondary particles with diameters of 5–20 μm, and the ball-like particles are made up of small primary particles with sizes of 200–500 nm (Fig. 2a and b). The surface of the bare $LiMn_{1/3}Ni_{1/3}Co_{1/3}O_2$ particles is smooth, as clearly shown in Fig. 2b. No distinct change of the particle size is observed after LiF modification. However, the surface of LiF-modified oxide particles becomes rough, and the distinct particle grains become fuzzy or disappear, as shown in Fig. 2d. It means that a thin LiF-modified layer forms on the surface of $LiMn_{1/3}Ni_{1/3}Co_{1/3}O_2$ particle, as shown in Fig. 3. In order to prove the homogeneity of the LiF-modified layer, EDS results are shown in Fig. 4. The F element in $LiMn_{1/3}Ni_{1/3}Co_{1/3}O_2$/LiF is uniformly distributed on the surface of the oxide particle, which is accordant with the result of SEM analysis.

The XPS spectra of bare $LiNi_{1/3}Co_{1/3}Mn_{1/3}O_2$ and $LiNi_{1/3}Co_{1/3}Mn_{1/3}O_2$/LiF are shown in Fig. 5. It clearly reveals that the $LiNi_{1/3}Co_{1/3}Mn_{1/3}O_2$/LiF has Mn 2p, Co 2p and Ni 2p peaks with remarkable chemical shift of binding energy, indicating that the Co, Ni and Mn ion environments change in the surface structure. It also indicates that the added LiF not only covers on the surface of $LiNi_{1/3}Co_{1/3}Mn_{1/3}O_2$ particles, but also has chemical bonding with the oxide. F^- may partly substitute O^{2-} of the surface lattice during annealing process. Such phenomenon was not distinctly observed when other fluorides such as ZrF_x, SrF_2, CaF_2 and LaF_3 were coated on the surface of oxides due to the large cations [38–40,46]. It seems that the small Li^+ in LiF facilitates the substitution of O^{2-} by F^- on the surface of oxide particle. It is also proved from the

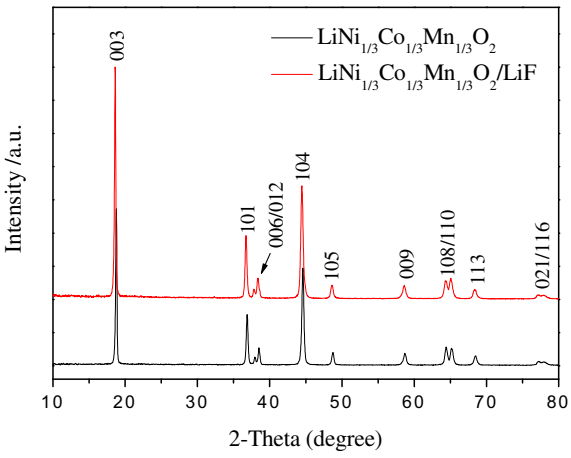

Fig. 1. XRD patterns of $LiNi_{1/3}Co_{1/3}Mn_{1/3}O_2$ and $LiNi_{1/3}Co_{1/3}Mn_{1/3}O_2$/LiF powders.

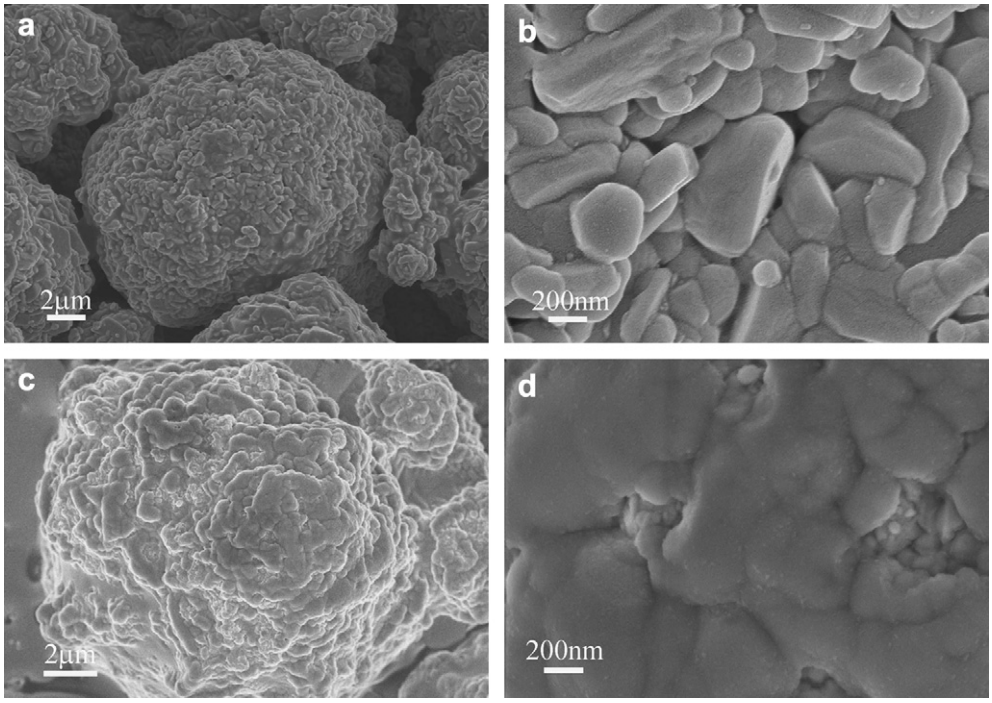

Fig. 2. SEM images of (a, b) $LiNi_{1/3}Co_{1/3}Mn_{1/3}O_2$ and (c, d) $LiNi_{1/3}Co_{1/3}Mn_{1/3}O_2$/LiF particles.

spectrum of F 1s. The binding energy of F 1s in LiF is 684.9 eV. However, in Fig. 5a, the peak of F 1s in $LiNi_{1/3}Co_{1/3}Mn_{1/3}O_2$/LiF shifts to 684.0 eV, indicating that there is chemical bonding between other elements and F. In addition, it is clear that the peak intensities of other elements decrease after LiF modification (Fig. 5b–e). In contrast, the shape of O 1s spectrum is changed a little. The chemical shift of the binding energy of O 1s implies that the oxygen environment in the surface structure of $LiNi_{1/3}Co_{1/3}Mn_{1/3}O_2$ is altered by the surface coating. The lower intensities of the O 1s peaks for the coated material imply that part of the fluoride formed on the surface is replaced by an oxide layer. The small and broad peak located at 531.5 eV in the spectrum is likely due to impurities with OH^- or O^- bonding on the surface [38]. The peak also presents after the coating, but its intensity reduces as shown in Fig. 5b. The red dashed is the result of peak separation. All the results confirm that the LiF-modified layer exists on the surface of $LiNi_{1/3}Co_{1/3}Mn_{1/3}O_2$ particles.

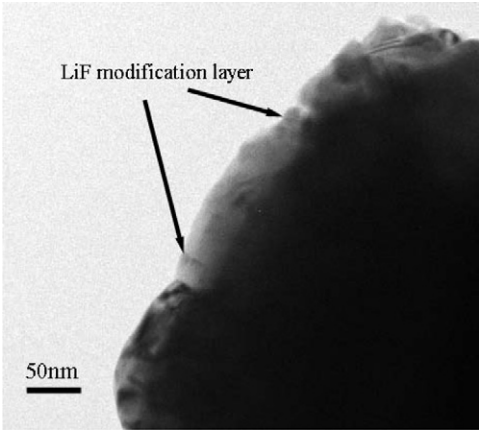

Fig. 3. A TEM image of $LiNi_{1/3}Co_{1/3}Mn_{1/3}O_2$/LiF particle.

3.2. Electrochemical properties

The initial charge–discharge curves of bare $LiNi_{1/3}Co_{1/3}Mn_{1/3}O_2$ and $LiNi_{1/3}Co_{1/3}Mn_{1/3}O_2$/LiF electrodes are shown in Fig. 6. The initial charge and discharge capacities are 221, 189.8 mAh g^{-1} and 222.5, 187.2 mAh g^{-1} for the bare $LiNi_{1/3}Co_{1/3}Mn_{1/3}O_2$ and $LiNi_{1/3}Co_{1/3}Mn_{1/3}O_2$/LiF at 0.1 C between 2.5 V and 4.5 V, respectively. The initial discharge capacity of bare oxide is a little higher than that of LiF-modified oxide. Fig. 7 shows the rate capability of bare $LiNi_{1/3}Co_{1/3}Mn_{1/3}O_2$ and $LiNi_{1/3}Co_{1/3}Mn_{1/3}O_2$/LiF between 2.5 V and 4.5 V at charge–discharge rates from 0.1 C to 10 C. The bare $LiNi_{1/3}Co_{1/3}Mn_{1/3}O_2$ has a higher initial discharge capacity than the LiF-modified oxide at 0.1 C. However, as the current density increases, the discharge capacity of bare $LiNi_{1/3}Co_{1/3}Mn_{1/3}O_2$ decreases rapidly, only 95 mAh g^{-1} at 10 C. The distinct decrease in discharge capacity of bare $LiNi_{1/3}Co_{1/3}Mn_{1/3}O_2$ is due to the slow kinetics at high rates and the destruction of the surface resulting from the side reactions between the active material and electrolyte [39]. When the discharge rate is back to 0.1 C, the bare $LiNi_{1/3}Co_{1/3}Mn_{1/3}O_2$ has a discharge capacity of 160 mAh g^{-1}, only about 83.6% discharge capacity left compared to that of the initial cycle at 0.1 C. For the $LiNi_{1/3}Co_{1/3}Mn_{1/3}O_2$/LiF electrode, it delivers a high discharge capacity of 137.7 mAh g^{-1} at 10 C, and has capacity retention of 97.2% with respect to the initial cycle at 0.1 C when the cell is discharged back to 0.1 C. The rate capability obtained here is much higher than those of $LiNi_{1/3}Co_{1/3}Mn_{1/3}O_2$ modified with other oxides [29,47,48] or fluorides [38–40] since these surface modifications with poor conductivity will certainly reduce the capacity at high discharge rates. The good rate capability of LiF-modified materials could be attributed to the existence of the strong bonding by F which stabilized the surface structure and increased the stability of electrode materials against HF attack at high discharge current densities [49,50]. Furthermore, surface F-substitution may modify the formation of SEI film to reduce the charge transfer resistance after activation at the beginning of the cycling. It can be proved in the following EIS tests.

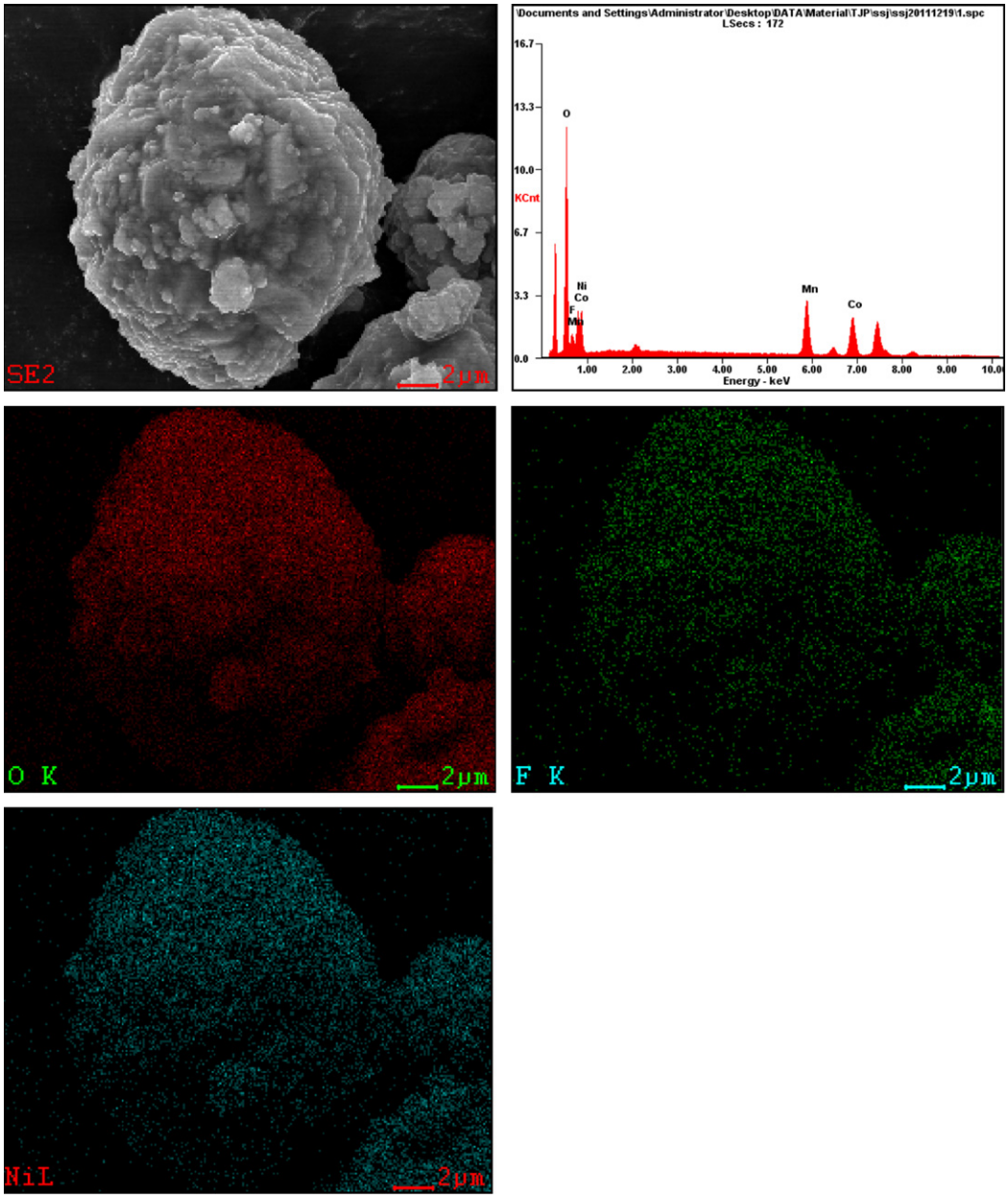

Fig. 4. EDS element maps of $LiNi_{1/3}Co_{1/3}Mn_{1/3}O_2$/LiF particle.

Fig. 8 shows the cyclic performances of bare $LiNi_{1/3}Co_{1/3}Mn_{1/3}O_2$ and $LiNi_{1/3}Co_{1/3}Mn_{1/3}O_2$/LiF at different charge–discharge rates. As shown in Fig. 8a, the $LiNi_{1/3}Co_{1/3}Mn_{1/3}O_2$/LiF delivers a discharge capacity of 181.6 mAh g^{-1} at 0.1 C after 50 cycles, only 3.0% discharge capacity lost. However, the bare $LiNi_{1/3}Co_{1/3}Mn_{1/3}O_2$ has a discharge capacity of 168.1 mAh g^{-1} after 50 cycles, with a capacity retention of 88.6%. The high capacity retention of $LiNi_{1/3}Co_{1/3}Mn_{1/3}O_2$/LiF is mainly due to the LiF-modified layer, which protects the layered oxide from attacking in electrolyte. The attacking of HF produced by $LiPF_6$ in the electrolyte is perfectly obstructed due to the modification layer on the surface of the particles [35,36]. It hinders the metal ions from dissolving in the electrolyte during the charge–discharge process. In order to give further evidence of the effect of LiF-modified layer at elevated charge–discharge current densities, cyclic performances at 1 C, 2 C, 5 C and 10 C are also carried out, as shown in Fig. 8a and b. After 50 cycles, the capacity retentions of bare $LiNi_{1/3}Co_{1/3}Mn_{1/3}O_2$ are 72.6%, 58.0%, 52.9% and 44.9% at 1 C, 2 C, 5 C and 10 C, respectively, while the capacity retentions of LiF-modified oxide are 91.1%, 92.8%, 85.9% and 78.7% at 1 C, 2 C, 5 C and 10 C, respectively, much higher than those of the bare one. It effectively proves that the LiF-modified layer also plays a significant role in the cyclic performance of layered oxide at elevated current density.

It is important for the application of lithium ion batteries at high or low temperatures. The electrochemical performances of $LiNi_{1/3}Co_{1/3}Mn_{1/3}O_2$ and $LiNi_{1/3}Co_{1/3}Mn_{1/3}O_2$/LiF electrodes at high or low temperatures are performed to evaluate the effect of LiF modification. Fig. 9a shows the rate capability of $LiNi_{1/3}Co_{1/3}Mn_{1/3}O_2$ before and after LiF modification at 0 °C from 0.1 C to 2 C. The bare $LiNi_{1/3}Co_{1/3}Mn_{1/3}O_2$ and $LiNi_{1/3}Co_{1/3}Mn_{1/3}O_2$/LiF deliver initial discharge capacities of 171.1 and 173.4 mAh g^{-1} at 0.1 C, respectively, which are a little lower than those obtained at room

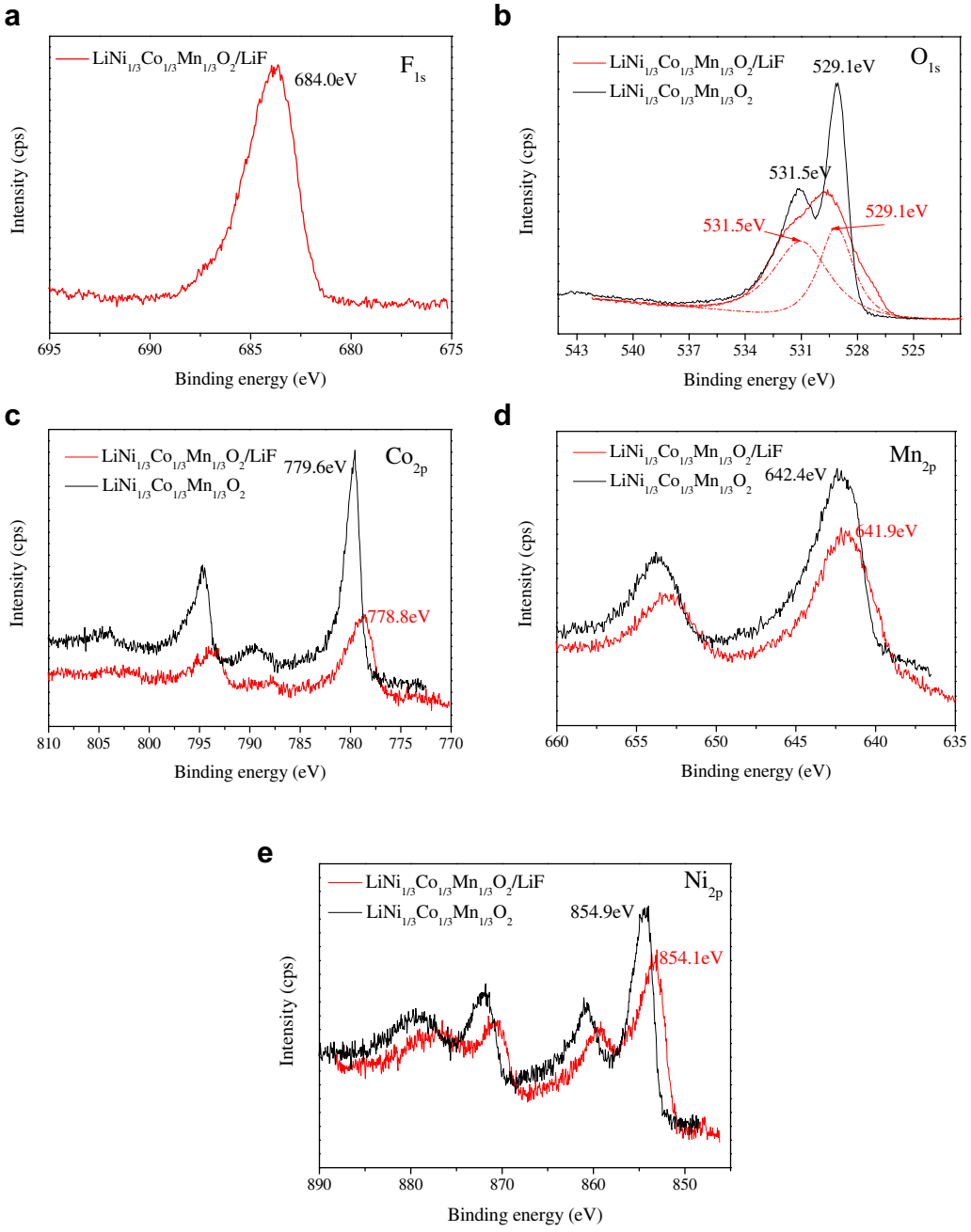

Fig. 5. XPS spectra of $LiNi_{1/3}Co_{1/3}Mn_{1/3}O_2$ and $LiNi_{1/3}Co_{1/3}Mn_{1/3}O_2$/LiF.

temperature. As the rate increases, the decrease in discharge capacity of LiF-modified oxide is much smaller than that of the bare one at low temperature. As shown in Fig. 9a, the $LiNi_{1/3}Co_{1/3}Mn_{1/3}O_2$/LiF has discharge capacities of 168.1 mAh g^{-1} at 0.2 C, 148.6 mAh g^{-1} at 0.5 C, 121.7 mAh g^{-1} at 1 C, 103.8 mAh g^{-1} at 1.5 C and 88.1 mAh g^{-1} at 2 C at 0 °C, much higher than the bare $LiNi_{1/3}Co_{1/3}Mn_{1/3}O_2$. It indicates that the LiF modification is effective at low temperature. The improvement of rate capability at low temperature can be attributed to the F-substituted surface which may lead to the better formation of SEI film with improved conductivity. Cyclic performance of both the electrodes at 0 °C is also performed at 0.1 C, 0.5 C and 1 C, as shown in Fig. 9b. The capacity retentions of 92.8%, 91.9% and 77% are obtained for the $LiNi_{1/3}Co_{1/3}Mn_{1/3}O_2$/LiF after 50 cycles at 0.1 C, 0.5 C and 1 C, respectively, much higher than those of the bare one. As the test temperature falls to −20 °C, the bare oxide and LiF-modified oxide can deliver a discharge capacity of 85.1 and 85.6 mAh g^{-1} at 0.1 C after activation for several cycles, respectively. And similar phenomenon can be observed that the LiF-modified oxide has high capacity retention of 95% after 50 cycles. Promoting the test temperature to 60 °C, the bare $LiNi_{1/3}Co_{1/3}Mn_{1/3}O_2$ and $LiNi_{1/3}Co_{1/3}Mn_{1/3}O_2$/LiF has a high initial discharge capacity of 185.3 and 182.4 mAh g^{-1} at 1 C, respectively. Furthermore, the LiF-modified oxide is much more stable at high temperature, about 93.5% discharge capacity retained after 50 cycles with respect to the initial cycle. It indicates that the LiF modification has distinct effect on the electrochemical performances of $LiNi_{1/3}Co_{1/3}Mn_{1/3}O_2$ not only at room temperature, but also at low and high temperatures.

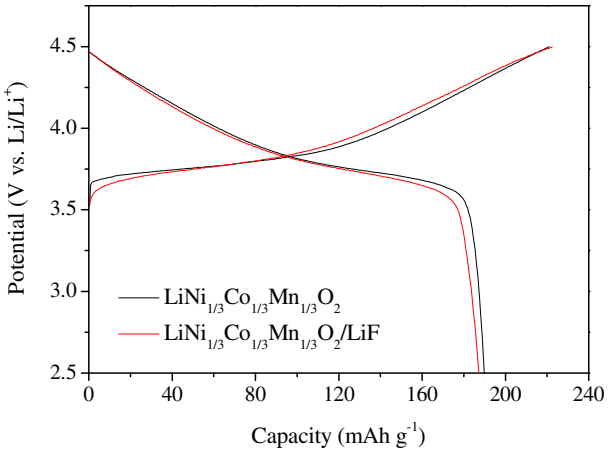

Fig. 6. Initial charge–discharge curves of $LiNi_{1/3}Co_{1/3}Mn_{1/3}O_2$ and $LiNi_{1/3}Co_{1/3}Mn_{1/3}O_2$/LiF electrodes at 0.1 C between 2.5 V and 4.5 V.

In order to further understand the effect of LiF modification, CV tests were carried out in this work. The initial, second and 50th cycle curves of bare $LiNi_{1/3}Co_{1/3}Mn_{1/3}O_2$ and $LiNi_{1/3}Co_{1/3}Mn_{1/3}O_2$/LiF are shown in Fig. 10. The cells were first tested in the potential window of 2.5–4.8 V at a scan rate of 0.1 mV s^{-1} for two cycles, they were then cycled at a charge-discharge rate of 1 C for 50 cycles. After cycling, the cells were again put on the electrochemical workstation and taken another CV curve. Fig. 10a shows the CV curves of bare $LiNi_{1/3}Co_{1/3}Mn_{1/3}O_2$. The main redox peaks appear at a potential range of 3.6 V–4.0 V. In addition, a small oxidation peak appears at about 4.6 V and a reduction peak at about 4.5 V for the first cycle. The first oxidation peak at 3.96 V corresponds to the oxidation of Ni^{2+}/Ni^{4+} couple and the second oxidation peak at 4.6 V corresponds to the oxidation of Co^{3+}/Co^{4+} couple. The reduction peak at 3.7 V is mainly associated with the reduction of the Ni^{4+}/Ni^{2+} couple and another weak peak at 4.55 V is ascribed to the reversible reaction at high potential [51,52]. The polarization of bare $LiNi_{1/3}Co_{1/3}Mn_{1/3}O_2$ decreases from 259 mV at the first cycle to 111 mV at the second cycle. This may be due to activation of the initial charge–discharge process. The CV curves of bare $LiNi_{1/3}Co_{1/3}Mn_{1/3}O_2$ during initial and second cycles exhibit highly symmetrical and sharp anodic/cathodic peaks. However, after 50 cycles at 1 C, the redox peaks of the CV curve become unsymmetrical and broad, the reduction peak nearly disappears. In addition, the polarization of the bare $LiNi_{1/3}Co_{1/3}Mn_{1/3}O_2$ increases to 341 mV, which indicates slow kinetics and poor electrochemical performances. Fig. 10b shows the CV curves of $LiNi_{1/3}Co_{1/3}Mn_{1/3}O_2$/LiF electrode. The results of first two cycles are similar to those of bare $LiNi_{1/3}Co_{1/3}Mn_{1/3}O_2$. The polarization of $LiNi_{1/3}Co_{1/3}Mn_{1/3}O_2$/LiF decreases from 200 mV at the first cycle to 100 mV at the second cycle. Highly symmetrical and sharper anodic/cathodic peaks can also be observed on the CV curve of $LiNi_{1/3}Co_{1/3}Mn_{1/3}O_2$/LiF after 50 cycles at 1 C. The polarization of the LiF-modified oxide increases to 291 mV, smaller than that of the bare one. And a clear reduction peak can be seen at 3.66 V after 50 cycles. The CV results of the $LiNi_{1/3}Co_{1/3}Mn_{1/3}O_2$/LiF are also accordant with the cyclic performance. Such good results are all attributed to the LiF-modified layer on the surface of the oxide particles, which reduces the dissolution of metal ions in the active material, and stabilizes the surface structure of the oxide during the charge–discharge process. In addition, the LiF modification probably improves the conductivity of the surface layer through the formation of SEI film.

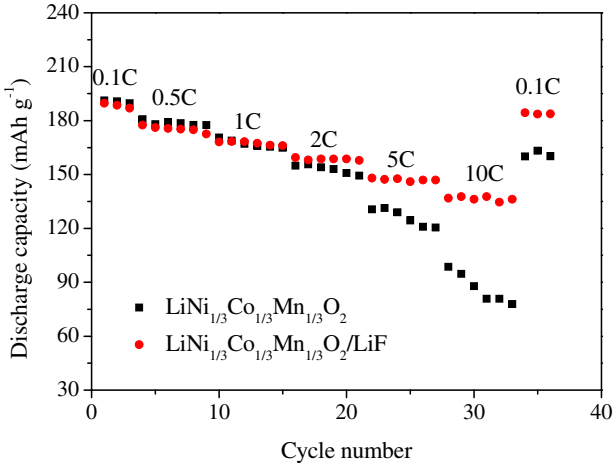

Fig. 7. Rate capability of $LiNi_{1/3}Co_{1/3}Mn_{1/3}O_2$ and $LiNi_{1/3}Co_{1/3}Mn_{1/3}O_2$/LiF from 0.1 C to 10 C in the voltage range of 2.5–4.5 V at room temperature.

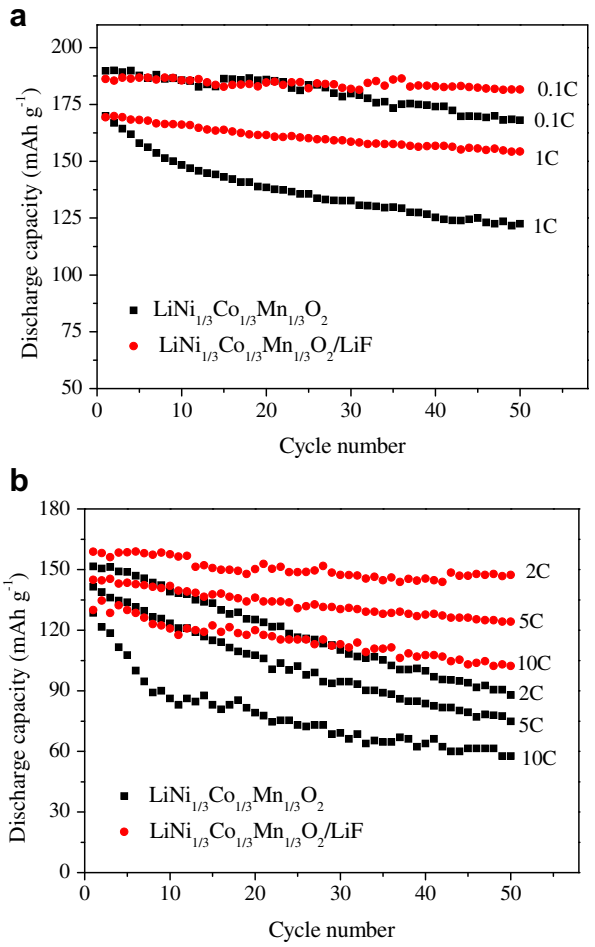

Fig. 8. Cycle performance of $LiNi_{1/3}Co_{1/3}Mn_{1/3}O_2$ and $LiNi_{1/3}Co_{1/3}Mn_{1/3}O_2$/LiF at (a) 0.1 C, 1 C and (b) 2 C, 5 C and 10 C between 2.5 V and 4.5 V for 50 cycles at room temperature.

Fig. 11 shows the Nyquist plots of bare $LiNi_{1/3}Co_{1/3}Mn_{1/3}O_2$ and $LiNi_{1/3}Co_{1/3}Mn_{1/3}O_2$/LiF at the charge state of 4.5 V in the first, 15th, 30th and 50th cycle. The shapes of the Nyquist plots are all similar. They are composed of a small interrupt and a small

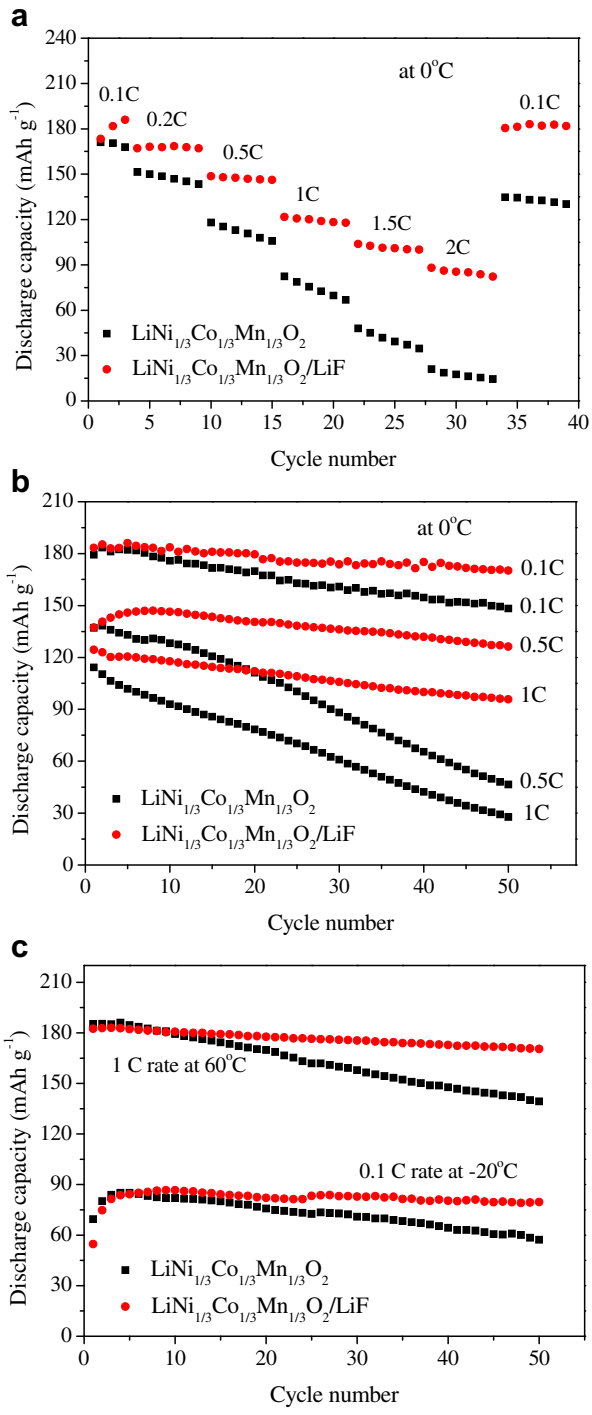

Fig. 9. (a) Rate capability of $LiNi_{1/3}Co_{1/3}Mn_{1/3}O_2$ and $LiNi_{1/3}Co_{1/3}Mn_{1/3}O_2$/LiF from 0.1 C to 2 C in the voltage range of 2.5–4.5 V at 0 °C, (b) cycle performance at 0.1 C, 0.5 C and 1 C at 0 °C, (c) cycle performance at −20 °C and 60 °C.

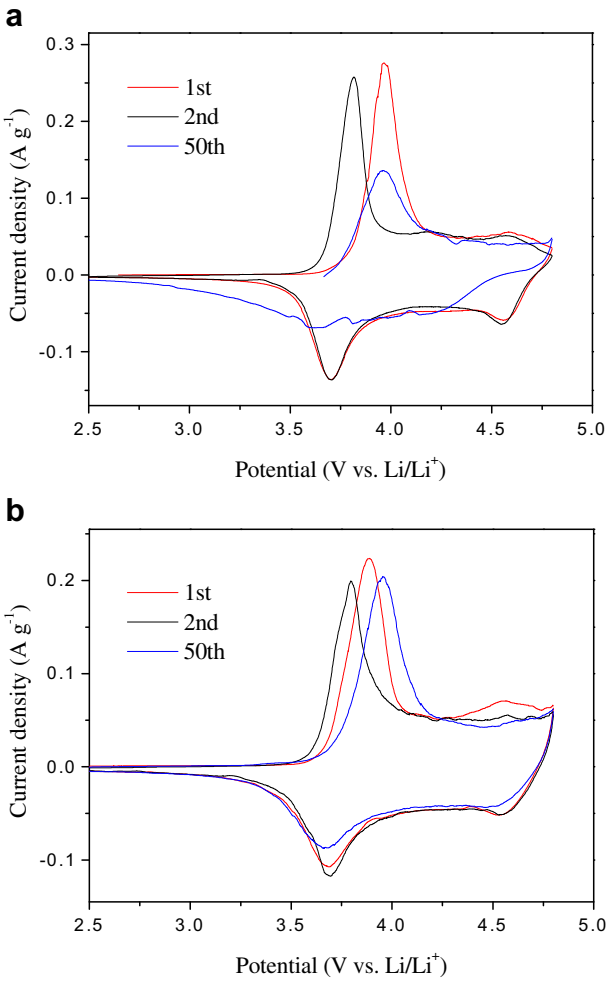

Fig. 10. CV curves of (a) $LiNi_{1/3}Co_{1/3}Mn_{1/3}O_2$ and (b) $LiNi_{1/3}Co_{1/3}Mn_{1/3}O_2$/LiF electrodes for the first, second and 50th cycles at a scan rate of 0.1 mV s^{-1}.

semicircle in the high frequency, a big semicircle in the high to medium frequency and a quasi-straight line in the low frequency. The small interrupt in the high frequency is almost the same for both the electrodes (Fig. 11a and b), which corresponds to the solution resistance R_e [53]. The small semicircle in the high frequency is assigned to the resistance (R_f) of Li^+ diffusion in the surface layer (including the SEI film and the surface-modified layer); and another semicircle in the high to medium frequency is assigned to the charge transfer resistance (R_{ct}). The equivalent circuit in Fig. 11c is used to fit the EIS data to give a quantitative result to further understand the effect of the modification layer. Many similar equivalent circuits are reported [29,54–56], and they are suitable to explore the Nyquist plots of electrode materials with a modification layer. CEP_f, CEP_{ct} and Z_w in Fig. 11c represent non-ideal capacitance of the surface layer, non-ideal capacitance of the double-layer and Warburg impedance which refers to the resistance of Li^+ diffusion in bulk material, respectively. The values of R_f and R_{ct} of bare $LiNi_{1/3}Co_{1/3}Mn_{1/3}O_2$ at the first cycle are 27 Ω and 39.7 Ω, respectively. As the charge-discharge process goes along, the values of R_f of both the electrodes first decrease and then increase just a little during all the cycle process. However, the value of R_{ct} of bare $LiNi_{1/3}Co_{1/3}Mn_{1/3}O_2$ increases so fast that the Warburg region (the quasi-straight line) becomes indistinguishable. The value of R_{ct} is 347.5 Ω after 50 cycles, much higher than that of the initial one.

The value of R_{ct} for $LiNi_{1/3}Co_{1/3}Mn_{1/3}O_2$/LiF after 50 cycles is only about 54.1 Ω, much smaller than that for the bare $LiNi_{1/3}Co_{1/3}Mn_{1/3}O_2$. The small increment in R_{ct} can be explained as followers: On one hand, the LiF modification stabilizes the surface structure of the layered oxide, thus the dissolution of metal ions is reduced. On the other hand, better SEI film forms due to the partly F-substitution which facilitates Li^+ to diffuse through. The EIS results again prove the effect of LiF modification on layered $LiMn_{1/3}Ni_{1/3}Co_{1/3}O_2$.

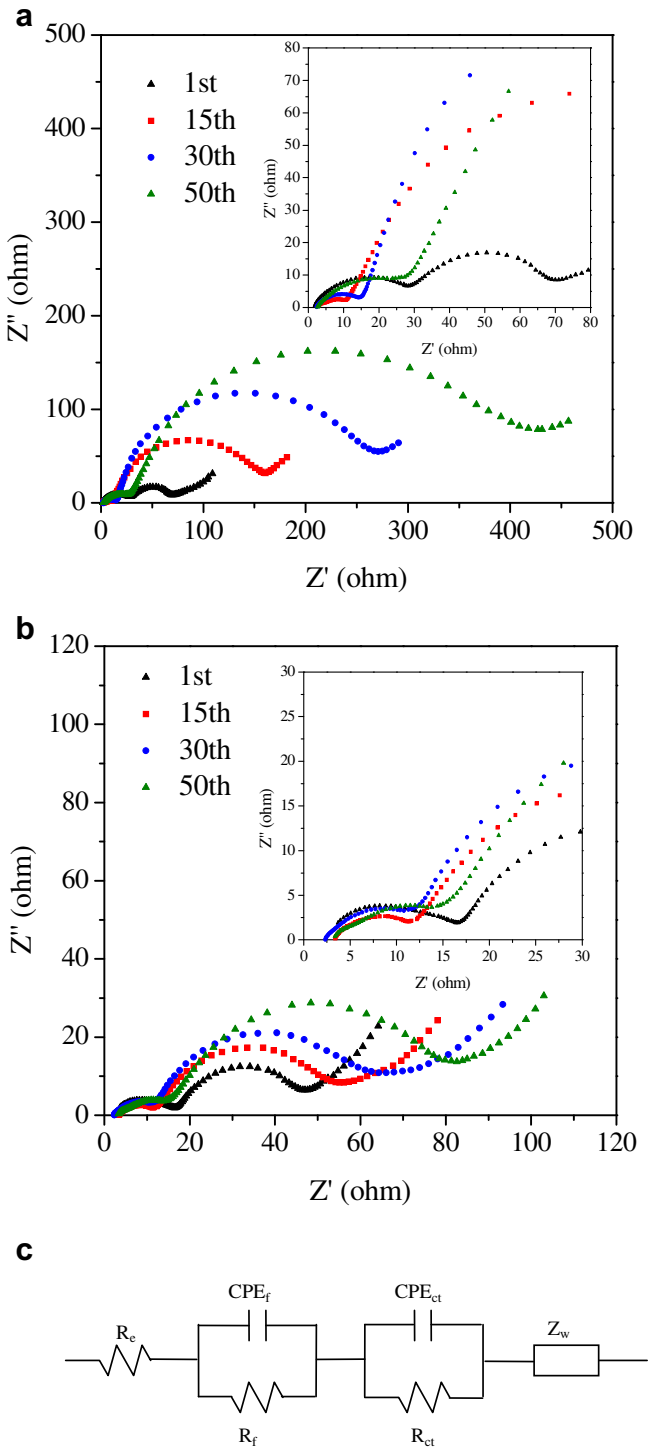

Fig. 11. Nyquist plots of (a) $LiNi_{1/3}Co_{1/3}Mn_{1/3}O_2$ and (b) $LiNi_{1/3}Co_{1/3}Mn_{1/3}O_2$/LiF electrodes at a charge state of 4.5 V for the first, 15th, 30th and 50th cycle, (c) equivalent circuit performed to fit the Nyquist plots in (a) and (b).

4. Conclusions

LiF was successfully used to modify the surface of $LiMn_{1/3}Ni_{1/3}Co_{1/3}O_2$ via a wet chemical process followed by an annealing process at 500 °C. XRD and XPS analysis indicate that the lattice structure of $LiNi_{1/3}Co_{1/3}Mn_{1/3}O_2$ is not changed after the surface modification and part of F^- dopes into the surface lattice of the oxide particles. The LiF-modified $LiMn_{1/3}Ni_{1/3}Co_{1/3}O_2$ exhibits a high capacity retention of 97.5% at 0.1 C after 50 cycles and a high initial discharge capacity of 137 mAh g^{-1} at 10 C at room temperature. Furthermore, the LiF modification is still effective at high or low temperatures. The improvement of cycle stability and rate capability can be attributed to the LiF-modified layer on $LiNi_{1/3}Co_{1/3}Mn_{1/3}O_2$, which not only strengthens the particle surface to reduce the dissolution of metal ions, but also enhances the conductivity of the surface layer through partly F-substitution. Therefore, the LiF modification will be an effective way for the application of layered oxide in lithium ion batteries.

Acknowledgments

This work is supported by Key Science and Technology Innovation Team of Zhejiang Province (2010R50013) and Fundamental Research Funds for the Central Universities (2011QNA4006).

References

[1] B. Markovsky, A. Rodkin, Y.S. Cohen, O. Palchik, E. Levi, D. Aurbach, H.J. Kim, M. Schmidt, J. Power Sources 119–121 (2003) 504.
[2] Y. Shao-Horn, S.A. Hackney, A.R. Armstrong, P.G. Bruce, R. Gitzendanner, C.S. Johnson, M.M. Thackeray, J. Electrochem. Soc. 146 (1999) 2404.
[3] T. Ohzuku, Y. Makimura, Chem. Lett. 7 (2001) 642.
[4] N. Yabuuchi, T. Ohzuku, J. Power Sources 119 (2003) 171.
[5] J.Q. Deng, L.J. Xi, L.H. Wang, Z.M. Wang, C.Y. Chung, X.D. Han, H.Y. Zhou, J. Power Sources 217 (2012) 491.
[6] S.K. Martha, J. Nanda, G.M. Veith, N.J. Dudney, J. Power Sources 216 (2012) 179.
[7] H.H. Zheng, L. Tan, G. Liu, X.Y. Song, V.S. Battaglia, J. Power Sources 208 (2012) 52.
[8] S.J. Shi, Y.J. Mai, Y.Y. Tang, C.D. Gu, X.L. Wang, J.P. Tu, Electrochim. Acta 77 (2012) 39.
[9] P. Manikandan, M.V. Ananth, T.P. Kumar, M. Raju, P. Periasamy, K. Manimaran, J. Power Sources 196 (2011) 10148.
[10] H.M. Wu, J.P. Tu, Y.F. Yuan, J.Y. Xiang, X.T. Chen, X.B. Zhao, G.S. Cao, J. Electroanaly. Chem. 608 (2007) 8.
[11] A.M.A. Hashem, A.E. Abdel-Ghany, A.E. Eid, J. Trottier, K. Zaghib, A. Mauger, C.M. Julien, J. Power Sources 196 (2011) 8632.
[12] Y.-J. Gu, Y.-B. Chen, H.-Q. Liu, Y.-M. Wang, C.-L. Wang, H.-K. Wu, J. Alloys Compd. 509 (2011) 7915.
[13] H.-G. Kim, S.-T. Myung, J.K. Lee, Y.-K. Sun, J. Power Sources 196 (2011) 6710.
[14] G.R. Li, X. Feng, Y. Ding, S.H. Ye, X.P. Gao, Electrochim. Acta 78 (2012) 308.
[15] Y. Xia, M. Yoshio, J. Electrochem. Soc. 143 (1996) 825.
[16] F. Wu, M. Wang, Y.F. Su, L.Y. Bao, S. Chen, J. Power Sources 195 (2010) 2900.
[17] H.B. Ren, X. Li, Z.H. Peng, Electrochim. Acta 56 (2011) 7088.
[18] A. Mahmoud, I. Saadoune, J.M. Amarilla, R. Hakkou, Electrochim. Acta 56 (2011) 4081.
[19] G.H. Kim, S.T. Myung, H.J. Bang, J. Prakash, Y.K. Suna, Electroche. Solid-State Lett. 7 (2004) A477.
[20] Y.J. Huang, D.S. Gao, G.T. Lei, Z.H. Li, G.Y. Su, Mater. Chem. Phys. 106 (2007) 354.
[21] H.S. Shin, D. Shin, Y.K. Sun, Electrochim. Acta 52 (2006) 1477.
[22] M. Kageyama, D. Li, K. Kobayakaw, Y. Sato, Y.S. Lee, J. Power Sources 157 (2006) 494.
[23] S.U. Woo, B.C. Park, C.S. Yoon, S.T. Myung, J. Prakash, Y.K. Sun, J. Electrochem. Soc. 154 (2007) A649.
[24] S. Jouanneau, J.R. Dahn, J. Electrochem. Soc. 151 (2004) A1749.
[25] M. Ménétrier, J. Bains, L. Croguennec, A. Flambard, E. Bekaert, C. Jordy, Ph. Biensan, C. Delmas, J. Solid State Chem. 181 (2008) 3303.
[26] D. Li, Y. Sasaki, K. Kobayabaw, H. Noguchi, Y. Sato, Electrochim. Acta 52 (2006) 643.
[27] G.H. Kim, M.H. Kim, S.T. Myung, Y.K. Sun, J. Power Sources 146 (2005) 602.
[28] S.H. Kang, K. Amine, J. Power Sources 146 (2005) 654.
[29] F. Wu, M. Wang, Y.F. Su, L.Y. Bao, S. Chen, Electrochim. Acta 54 (2009) 6803.
[30] S.K. Hu, G.H. Cheng, M.Y. Cheng, B.J. Hwang, R. Santhanam, J. Power Sources 188 (2009) 564.
[31] S.J. Shi, J.P. Tu, Y.J. Mai, Y.Q. Zhang, C.D. Gu, X.L. Wang, Electrochim. Acta 63 (2012) 112.
[32] Y.W. Zeng, J.H. Heb, J. Power Sources 189 (2009) 519.
[33] S.H. Lee, B.K. Koo, J.C. Kim, K.M. Kim, J. Power Sources 184 (2008) 276.
[34] J.T. Lee, F.M. Wang, C.S. Cheng, C.C. Li, C.H. Lin, Electrochim. Acta 55 (2010) 4002.
[35] Z.H. Chen, J.R. Dahn, Electrochem. Solid-State Lett. 7 (2004) A11.
[36] Z.H. Chen, J.R. Dahn, Electrochim. Acta 49 (2004) 1079.
[37] H.C. Lin, J.M. Zheng, Y. Yang, Mater. Chem. Phys. 119 (2010) 519.
[38] S.H. Yun, K.S. Park, Y.J. Park, J. Power Sources 195 (2010) 6108.
[39] J.G. Li, L. Wang, Q. Zhang, X.M. He, J. Power Sources 190 (2009) 149.

[40] K. Xu, Z.F. Jie, R.H. Li, Z.X. Chen, S.T. Wu, J.F. Gu, J.Z. Chen, Electrochim. Acta 60 (2012) 130.
[41] Y. Bai, C. Wu, F. Wu, Trans. Nonferrous Met. Soc. China 17 (2007) S892.
[42] L. Zhang, H. Noguchi, M. Yoshio, J. Power Sources 110 (2002) 57.
[43] H. Kobayashi, H. Sakaebe, H. Kageyama, K. Tatsumi, Y. Arachi, T. Kamiyama, J. Mater. Chem. 13 (2003) 590.
[44] D.C. Li, T. Muta, L.Q. Zhang, M. Yoshio, H. Noguchi, J. Power Sources 132 (2004) 150.
[45] B.J. Hwang, Y.W. Tsai, D. Carlier, G. Ceder, Chem. Mater. 15 (2003) 3676.
[46] Z.X. Yang, Q.D. Qiao, W.S. Yang, Electrochim. Acta 56 (2011) 4791.
[47] F. Wu, M. Wang, Y.F. Su, S. Chen, J. Power Sources 189 (2009) 743.
[48] Y.Y. Huang, J.T. Chen, F.Q. Cheng, W. Wan, W. Liu, H.H. Zhou, X.X. Zhang, J. Power Sources 195 (2010) 8267.
[49] S.W. Oh, S.H. Park, J.H. Kim, Y.C. Bae, Y.K. Sun, J. Power Sources 157 (2006) 464.
[50] Y.S. He, L. Pei, X.Z. Liao, Z.F. Ma, J. Fluorine Chem. 128 (2007) 139.
[51] M.M. Ma, N.A. Chernov, B.H. Toby, P.Y. Zavalij, M.S. Whittingham, J. Power Sources 165 (2007) 517.
[52] F. Wu, M. Wang, Y.F. Su, S. Chen, B. Xu, J. Power Sources 191 (2009) 628.
[53] Y.Q. Qiao, X.L. Wang, Y. Zhou, J.Y. Xiang, D. Zhang, S.J. Shi, J.P. Tu, Electrochim. Acta 56 (2010) 510.
[54] J. Liu, Q.Y. Wang, B. Reeja-Jayan, A. Manthiram, Electrochem. Commun. 12 (2010) 750.
[55] Y.Q. Qiao, J.P. Tu, X.L. Wang, D. Zhang, J.Y. Xiang, Y.J. Mai, C.D. Gu, J. Power Sources 196 (2011) 7715.
[56] J.P. Zhou, J.P. Tu, L.Y. Cheng, S.J. Shi, Y.Q. Qiao, W.L. Liu, X.L. Wang, C.D. Gu, J. Electrochem. Soc. 158 (2011) A1237.